Implementation of Adapted Black Box Models for the Performance Characterization of Commercial Sorption Chillers

Amín Altamirano[1*], Charles Maragna[2] and Brice Tremeac[1]

[1] Laboratoire du froid et des systèmes énergétiques et thermiques (Lafset), Conservatoire national des arts et métiers, Paris (France)

[2] Bureau de Recherches Géologiques et Minière (BRGM), Orléans (France)

Abstract

Thermally-driven sorption chillers represent an excellent alternative to make use of low-temperature renewable energy sources such as solar or geothermal energy in the range of 60-120°C. In these cases, three commercially available geometries emerge: two closed sorption systems (single-stage absorption and adsorption chillers) and an open sorption system (Dissociative Evaporative Cooling system, DEC). Due to the complexity of these systems, their modeling (which is fundamental for viability studies) remains a complicated task. In this regard, black box models represent a simple alternative to simulate their performance. Two specially adapted methods have been used in the literature for the most common system (the absorption chiller): the adapted characteristic equation (CE) and the Carnot function model (CFM). The present work studies the implementation of these methods with different commercial sorption chillers and discusses their advantages and their limits regarding each technology. The feasibility of the implementation of the CFM and the adapted CE method with adsorption chillers and DEC systems is demonstrated. Despite its natural advantages, the CFM presented the highest deviations (especially with $\dot{Q}_e$ and $\dot{Q}_g$), the reason behind this might be that the COP_{carnot} is a physical parameter that cannot be fitted (as in the case of the $\Delta\Delta t$' of the adapted CE method).

Keywords: sorption chiller, absorption chiller, adsorption chiller, DEC, black box, characteristic equation, Carnot function

1. Introduction

Given the current increase in the global energy demand related to cooling in the building sector, especially in tropical climates (IEA, 2018), the use of chillers that make use of renewable energy is becoming a necessity more than an option (Altamirano et al., 2019a). In this regard, thermally-driven sorption chillers represent an excellent alternative since these systems can make use of a renewable heat source (such as solar energy) to operate. These systems can be divided into two categories: closed cycle (in which the refrigerant fluid is not in direct contact with the air to be cooled, i.e., absorption and adsorption systems) and open cycle (in which the refrigerant fluid is in direct contact with the cooled air, i.e., Dissociative Evaporative Cooling systems). In terms of market penetration, among the thermally-driven systems, absorption chillers have the largest market share (82-84%), followed by adsorption (9-11%) and DEC systems (7%), respectively (Almasri et al., 2022).

The modeling of sorption systems is of fundamental importance for the evaluation of their performance, and in particular when they are coupled to other systems with variable requirements and availabilities (e.g., buildings, storage systems, and ambient source) (Altamirano et al., 2019b). Depending on the degree of physical insight on the machine, the different models can be divided into three categories: white box (physical), when it contains a complete insight into the physical phenomena in the system; gray box (semi-empirical), when there is some degree of physical insight, and black box, when no physical insight is required and the model is based on a dataset of experimental results In cases in which the potential of sorption chillers is to be estimated, no need for understanding the physical phenomena inside the machine is required and therefore, black box models are seem like the most suitable tool for these machines' modeling given their simplicity, accuracy, and ease of

Selection and/or peer review under responsibility of Scientific Committee
doi:10.18086/eurosun.2022.16.01 Available at http://proceedings.ises.org

implementation with different dynamic thermal simulation programs such as TRNSYS.

Among the black box model possibilities, there are two options that might be especially useful in the modeling of sorption systems: the adapted characteristic equation (CE) method and the Carnot function model (CFM). Indeed, these modeling methods use parameters function of the thermal sources' temperatures (commonly used by researchers and manufacturers for their characterization) to situate the different machine operating regimes. These modeling methods, however, have only been studied in the context of absorption chillers (Altamirano et al., 2021). Nevertheless, the characterization of the other sorption chillers' options is also required to compare the different available solutions.

The present work consists of the modeling of commercial thermally driven sorption chillers (a single-stage absorption chiller, a single-stage adsorption chiller, and a DEC system) through the adapted CE and CFM methods. The study is divided into three parts. In the first part, a theoretical description of the studied systems, their operating conditions, and the performance evaluation parameters is presented. The following section describes the black box modeling methods used. Finally, the modeling results and the prediction accuracy of the different models on the selected systems are presented and discussed.

2. Operating conditions and performance evaluation parameters

Sorption systems make use of a physical or chemical affinity between two substances to generate cooling thanks to a heat source. One of these substances plays the role of the refrigerant, whereas the other one, with lower volatility, plays the role of the sorbent. The most general case (the case of closed systems) is represented by a theoretical machine with three heat sources at different temperature levels (Figure 1). In such a case, there is a component commonly named as desorber or generator, that receives heat ($\dot{Q}_g$) from a high-temperature source (T_g). There are also components, called condenser and ad/absorber, that reject heat ($\dot{Q}_{int}$) to a source that is at an intermediate temperature level (T_{int}). Finally, there is a component (an evaporator) that extracts heat ($\dot{Q}_e$) from a low temperature source (T_e). Different geometrical configurations are available for commercial closed-cycle sorption systems. However, the single-effect configuration is the most adapted for low-temperature renewable energy sources such as solar or geothermal energy in the range of 60-120°C (obtained through flat plate and evacuated tube collectors) (Alahmer and Ajib, 2020). In the case of open-cycle sorption systems, the most commonly manufactured system is based on the Pennington cycle (also known as ventilation cycle) (La et al., 2010), which is also adapted to similar driving temperature levels (Almasri et al., 2022). Taking this into consideration, three sorption chillers with a similar nominal capacity were selected: a 35-kW single-effect commercial absorption chiller (Yazaki Energy Systems Inc., 2018), a 30-kW single-effect commercial adsorption chiller (InvenSor GmbH, 2015), and a 20-kW DEC experimental system (Pons and Kodama, 1999) with similar nominal conditions than commercial systems (Robatherm GmbH, 2014).

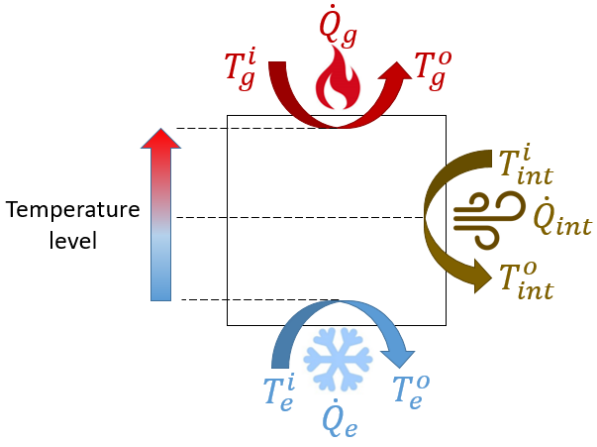

Fig. 1: Illustrative diagram of a sorption machine with three heat sources at different temperature levels.

The nominal and part-load operation range conditions of the selected systems are presented in Table 1. The data of the commercial systems (absorption and adsorption chiller) were extracted from the commercial catalogues (InvenSor GmbH, 2015; Yazaki Energy Systems Inc., 2018), whereas the data of the DEC system were obtained

from (Pons and Kodama, 1999). After the discretization and extraction of these data, the total number of operating conditions are 358, 28, and 9 for the absorption chiller, adsorption chiller, and DEC system, respectively.

Tab. 1: Operation range conditions of the studied systems (nominal conditions in parentheses) (InvenSor GmbH, 2015; Pons and Kodama, 1999; Yazaki Energy Systems Inc., 2018)

Variable	35-kW H_2O-LiBr Absorption Chiller	30-kW H_2O-Zeolite Adsorption Chiller	20-kW H_2O-Silica Gel DEC System
T_e^o $[°C]$	5 – 12 (7)	10 – 17.4 (14)	– (14)
$\dot{Q}_e$ $[kW]$	2.9 – 60.7 (35.2)	4.5 – 33.9 (29.5)	16 – 22.9 (20.2)
T_{int}^i $[°C]$	24 – 32 (31)	22 – 37 (27)	– (31)
$\dot{Q}_{int}$ $[kW]$	13.7 – 148.3 (85.4)	15.4 – 93.7 (78.5)	16 – 23 (20.2)
T_g^i $[°C]$	75 – 95 (88)	45 – 95 (85)	62 – 100.8 (80.4)
$\dot{Q}_g$ $[kW]$	10.9 – 87.7 (50.2)	10.2 – 59.8 (49)	30.9 – 63.1 (37.9)
COP_{th} $[-]$	0.26 – 0.8 (0.7)	0.39 – 0.68 (0.6)	0.36 – 0.54 (0.53)
COP_{carnot} $[-]$	1.24 – 4.58 (1.84)	1.22 – 6.77 (3.58)	1.56 – 3.15 (2.36)

The performance of sorption chillers depends on a large series of parameters that can be internal (the working fluid, the exchanger technology, or the control system) or external (the climatic conditions or the thermodynamic state of the heat transfer fluid) (Pons et al., 2012). Whereas the performance of mechanical compression machines is measured by the so-called electrical coefficient of performance (COP) (the cooling capacity divided by the electrical input to the compressor, defined by equation 1, in the case of sorption machines, because the driving source is heat, a thermal COP is often used, defined by equation 2. Moreover, some authors consider a global COP (equation 3), in which the heat source and the electrical supply (e.g., in the case of using pumps) are taken into account as energy sources.

$$COP_{el} = \frac{\dot{Q}_e}{\dot{W}_{el}} \quad \text{(eq. 1)}$$

$$COP_{th} = \frac{\dot{Q}_e}{\dot{Q}_g} \quad \text{(eq. 2)}$$

$$COP_{gl} = \frac{\dot{Q}_e}{\dot{Q}_g + \dot{W}_{el}} \quad \text{(eq. 3)}$$

Another important parameter in the study of thermodynamic systems is the Carnot COP (equation 4), which represents the COP of an ideal cycle, and which is a function of the temperatures of the sources at the three levels in the case of closed-cycle sorption machines. The COP_{carnot}, therefore, implies a reversible process with infinite (isothermal) energy sources, which for the heat transfer fluids corresponds to the temperatures at the generator inlet (T_g^i), at the ad/absorber and condenser inlet ($T_a^i = T_c^i = T_{int}^i$), and at the evaporator outlet (T_e^o). This definition is particularly suitable since manufacturers of closed-cycle sorption machines use the same temperatures to characterize their systems. DEC machines, unlike closed-cycle systems, do not have an intermediate temperature source and a cold temperature source in the strict sense. Pons and Kodama (1999) propose to use the ambient temperature as the intermediate temperature source and the conditioned air temperature as the low-temperature source for the calculation of the Carnot COP.

$$COP_{carnot} = \left(\frac{T_g^i - T_{int}^i}{T_g^i}\right)\left(\frac{T_e^o}{T_{int}^i - T_e^o}\right) \quad \text{(eq. 4)}$$

3. Adapted black box modeling methods

3.1. Adapted characteristic equation method

The adapted CE method (Kühn and Ziegler, 2005) is based on a multiple linear regression to obtain an arbitrary parameter, called the adapted characteristic temperature difference ($\Delta\Delta t'$, equation 5), which is a function of the external source temperatures (at the evaporator, generator, and heat sink) linearly correlated with the cooling power (equation 6). A second fitting is then employed to correlate the $\Delta\Delta t'$ to the thermal power of the generator (equation 7). The authors of the original method propose the use of the external arithmetic mean temperatures of the heat sources, however, an alternative is the use of the generator inlet temperature (T_g^i), heat sink inlet temperature (T_{int}^i), and evaporator outlet temperature (T_e^o), since these variables are commonly used to characterize the part-load behavior of sorption chillers (experimental prototypes and commercial machines).

$$\Delta\Delta t' = T_g^i - a \cdot T_{int}^i + e \cdot T_e^o \quad \text{(eq. 5)}$$

$$\dot{Q}_e^{ce\prime} = s' \cdot \Delta\Delta t' + r = s' \cdot T_g^i - s' \cdot a \cdot T_{int}^i + s' \cdot e \cdot T_e^o + r \quad \text{(eq. 6)}$$

$$\dot{Q}_g^{ce\prime} = b \cdot \Delta\Delta t' + c \quad \text{(eq. 7)}$$

3.2. Carnot function model

The Carnot function model (Boudéhenn et al., 2014), on the other hand, characterizes the thermal COP and cooling capacity of the system in terms of its Carnot COP (equation 8) through fitted parameters $\omega_1, \omega_2, \tau_1, \tau_2$, and F_0.

$$F^{cfm} = \omega_1 \cdot e^{(-COP_{carnot}/\tau_1)} + \omega_2 \cdot e^{(-COP_{carnot}/\tau_2)} + F_0 \quad \text{(eq. 8)}$$

4. Results and discussion

The present section shows the results of the implementation of the two black box modeling methods presented in section 3 to the three selected sorption chillers. The least squares method along with the generalized reduced gradient (GRG) nonlinear method were used to fit the parameters of the equations presented in section 3 to the data of the different machines. The fitted parameters of the adapted CE method are presented in Table 2, whereas those of the CFM are presented in Table 3.

Tab. 2: Fitted parameters of the adapted CE method

	35-kW H_2O-LiBr Absorption Chiller	**30-kW H_2O-Zeolite Adsorption Chiller**	**H_2O-Silica Gel DEC System**
s'	1.46	0.61	0.16
a	2.13	2.24	4.73
e	0.41	1.42	2.95
r	-2.79	0.55	23.78
b	1.96	0.96	0.70
c	-0.79	3.78	60.35

As previously mentioned, the main advantage of the adapted CE method and the CMF with sorption chillers is that they have a specific parameter that represents the operating regime of the machine. In other words, they correlate either the $\Delta\Delta t'$ (equation 5) or the COP_{carnot} (equation 4) to the cooling power that the machine can deliver under certain conditions of specific source temperatures (T_e, T_{int}, and T_g) and at the same time, they give information about the thermal performance related to those operating conditions. In the case of the adapted CE method, the influence of the external temperatures on the operating regime is represented by the factors 1, a, and e in equation 5 for T_g^i, T_{int}^i, and T_e^o, respectively. Table 1 shows that for the three selected systems, T_{int}^i has the highest influence, followed by T_e^o, with exception of the absorption chiller, for which T_e^o seems to have the lowest influence on the operating regime. The COP_{carnot}, being a physical parameter, cannot be adjusted to better divide

the effects of the external temperatures. However, from its definition (equation 4), T_{int}^{i} has a strong influence on the system's operating regime, especially at low values of T_{int}^{i}.

Tab. 3: Fitted parameters of the CFM

	35-kW H2O-LiBr Absorption Chiller		30-kW H2O-Zeolite Adsorption Chiller		H2O-Silica Gel DEC System	
	$\dot{Q}_e^{cfm}$	COP_{th}^{cfm}	$\dot{Q}_e^{cfm}$	COP_{th}^{cfm}	$\dot{Q}_e^{cfm}$	COP_{th}^{cfm}
ω_1	-75.07	-2.69	-173.59	-1.46	-49.52	-2.84
ω_2	-90.11	-4.46*10^{12}	-38.39	-4.48*10^{12}	-29.64	-4.52*10^{12}
τ_1	1.18	0.38	65.82	0.64	0.60	0.10
τ_2	1.18	0.04	1.18	0.021	0.64	0.03
F_0	61.43	0.71	187.60	0.62	22.56	0.45

The modeling results of the implementation of the (a) CFM and the (b) adapted CE method to the absorption chiller are presented in Figure 2. Figure 2a shows that even in the COP_{th} prediction of the CFM seems to be good, the cooling load does not follow the same evolution as the proposed function. This happens especially for chilled water temperatures that are either very low or very high. On the other hand, even though the adapted CE method seems to properly predict the behavior of the cooling and heat source loads, there are some regimes at elevated values of $\Delta\Delta t'$ that do not correspond to the proposed function. Again, these conditions correspond to low evaporator temperatures, for which the performance of the chiller decreases drastically.

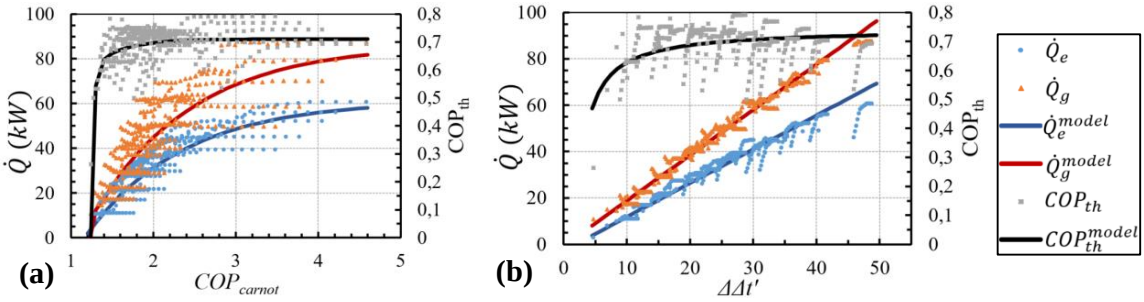

Fig. 2: Results of the implementation of the (a) CFM and the (b) adapted CE method with the absorption chiller

Figure 3 presents the comparison of the numerical results with the catalog data of the absorption chiller. $\dot{Q}_e^{cfm}$ has a coefficient of determination (R^2, useful to quantify the quality of the prediction of the model) of 0.8188, an average error of 17%, and 34.64% of the cooling loads that are predicted within an error of 10% or less (Figure 3a). Regarding $\dot{Q}_g^{cfm}$ (directly calculated having COP_{th}^{cfm} and $\dot{Q}_e^{cfm}$), it has a coefficient of determination of 0.7038, an average error of 19.22%, and 28.49% of the heat source loads that are predicted within an error of 10% or less (Figure 3b). Finally, regarding COP_{th}^{cfm}, it has a coefficient of determination of 0.2918, an average error of 6.12%, and 85.20% of the thermal COPs that are predicted within an error of 10% or less (Figure 3c).

$\dot{Q}_e^{ce\prime}$ has a coefficient of determination of 0.9485, an average error of 7.35%, and 70.95% of the cooling loads that are predicted within an error of 10% or less (Figure 3a). Regarding $\dot{Q}_g^{ce\prime}$, it has a coefficient of determination of 0.9767, an average error of 5.42%, and 88.27% of the heat source loads that are predicted within an error of 10% or less (Figure 3b). Finally, regarding $COP_{th}^{ce\prime}$ (directly calculated having $\dot{Q}_e^{ce\prime}$ and $\dot{Q}_g^{ce\prime}$), it has a coefficient of determination of 0.0861, an average error of 7.03%, and 78.21% of the thermal COPs that are predicted within an error of 10% or less (Figure 3c).

Figure 3a shows that the CFM has the largest prediction errors on the cooling load, especially at low operating regimes. It would seem from this figure that the COP_{carnot} has indeed some correlation with the cooling load. However, this correlation might not be good enough to be used in a performances prediction model. On the other

hand, the adapted CE method shows a good accuracy at low operating regimes and higher errors at high cooling loads, indicating that the hypothesis of a linear correlation of $\Delta\Delta t'$ with the cooling load might not be valid at these conditions. Similar results are observed for the comparison of the heat source load (Figure 3b). The adapted CE method, however, possesses low deviations in the whole range of operating conditions. The thermal COP is commonly overestimated by the models (Figure 3c). This might be due to missing data of the system operating at low performances (especially at heat source temperatures lower than 75°C). For a big part of the operating conditions, the machine operates with a COP_{th} close to the nominal one (0.7). Indeed, 70% of the operating conditions present a thermal COP between 0.65 and 0.75.

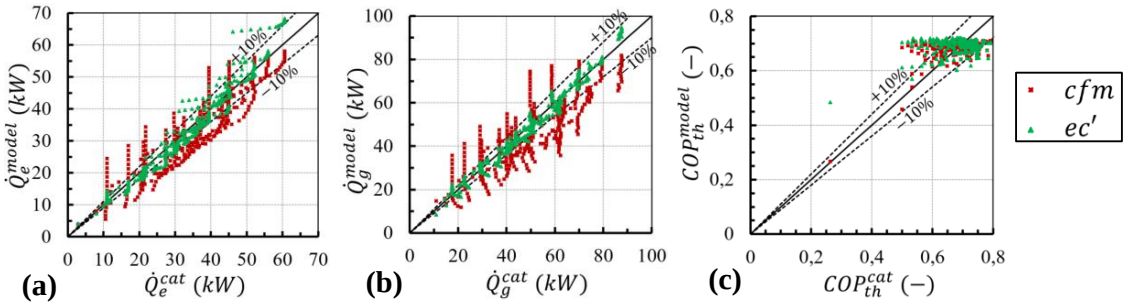

Fig. 3: Comparison between numerical and catalog results for the absorption chiller

The modeling results of the implementation of the (a) CFM and the (b) adapted CE method to the adsorption chiller are presented in Figure 4. To the best of our knowledge, this is the first time that these methods are applied to an adsorption chiller, and the results seem coherent and similar to those obtained with the absorption chiller.

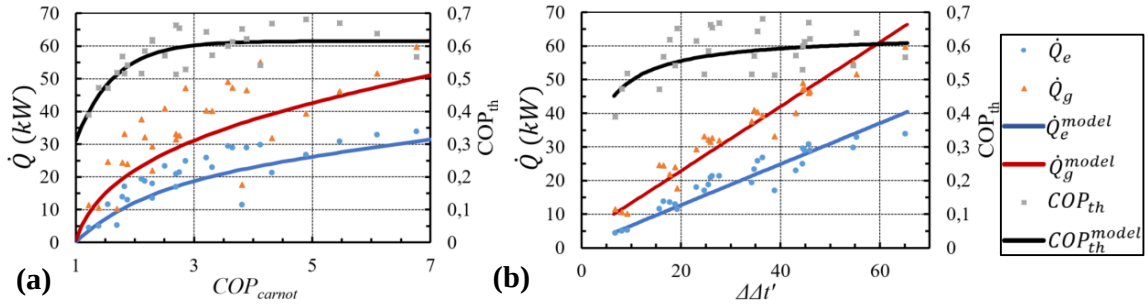

Fig. 4: Results of the implementation of the (a) CFM and the (b) adapted CE method with the adsorption chiller

Figure 5 presents the comparison of the numerical results with the catalog data of the adsorption chiller. $\dot{Q}_e^{cfm}$ has a coefficient of determination of 0.7590, an average error of 24.41%, and 14.29% of the cooling loads that are predicted within an error of 10% or less (Figure 5a). Regarding $\dot{Q}_g^{cfm}$, it has a coefficient of determination of 0.6207, an average error of 26.16%, and 14.28% of the heat source loads that are predicted within an error of 10% or less (Figure 5b). Finally, regarding COP_{th}^{cfm}, it has a coefficient of determination of 0.6379, an average error of 6.16%, and 85.71% of the thermal COPs that are predicted within an error of 10% or less (Figure 5c).

$\dot{Q}_e^{ce\prime}$ has a coefficient of determination of 0.8830, an average error of 13.44%, and 39.29% of the cooling loads that are predicted within an error of 10% or less (Figure 5a). Regarding $\dot{Q}_g^{ce\prime}$, it has a coefficient of determination of 0.94, an average error of 10.25%, and 57.14% of the heat source loads that are predicted within an error of 10% or less (Figure 5b). Finally, regarding $COP_{th}^{ce\prime}$, it has a coefficient of determination of 0.3365, an average error of 8.28%, and 50% of the thermal COPs that are predicted within an error of 10% or less (Figure 5c).

Similar to the case of the absorption chiller, the CFM presents the largest prediction errors on the cooling and heat source loads (Figures 5a and b). However, it has a higher precision on the thermal COP prediction (Figure 5c). For this machine, 42.86% of the operating conditions present a thermal COP between 0.55 and 0.65 (close to the nominal COP_{th} of 0.6). More information on the behavior of the machine at low operating performances is necessary for more accurate models.

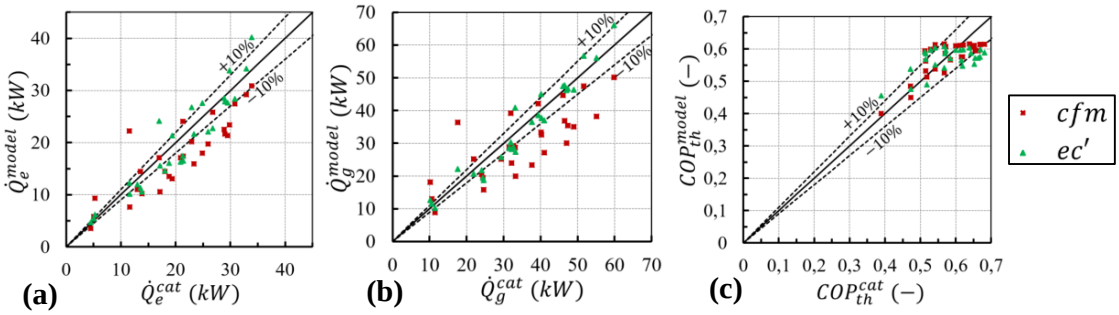

Fig. 5: Comparison between numerical and catalog results for the adsorption chiller

The modeling results of the implementation of the (a) CFM and the (b) adapted CE method to the DEC system are presented in Figure 6. To the best of our knowledge, this is the first time that these methods are applied to a DEC system and, from these figures, it seems that the CFM (Figure 6a) is well adapted to predict the cooling load of this system, however, this is not the case for the thermal COP, for which the model seems to have important deviations. One has to consider, however, that only 9 experimental conditions are available and therefore, the model prediction accuracy is highly dependent on the choice of said conditions. The adapted CE method seems to accurately predict the behavior of the DEC system (Figure 6b).

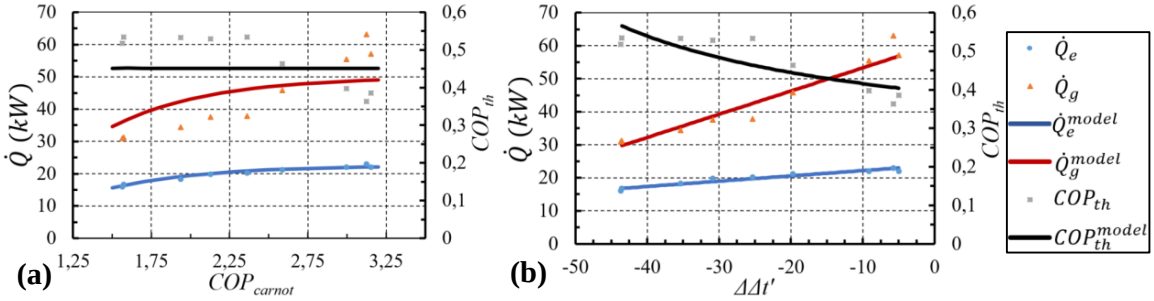

Fig. 6: Results of the implementation of the (a) CFM and the (b) adapted CE method with the DEC system

Figure 7 presents the comparison of the numerical results with the experimental data of the DEC system. $\dot{Q}_e^{cfm}$ has a coefficient of determination of 0.9602, an average error of 1.90%, and 100% of the cooling loads that are predicted within an error of 10% or less (Figure 7a). Regarding $\dot{Q}_g^{cfm}$, it has a coefficient of determination of 0.7136, an average error of 16.49%, and 11.11% of the heat source loads that are predicted within an error of 10% or less (Figure 7b). Finally, regarding COP_{th}^{cfm}, it has a coefficient of determination of 0.1760, an average error of 14.58%, and 11.1% of the thermal COPs that are predicted within an error of 10% or less (Figure 5c).

$\dot{Q}_e^{ce\prime}$ has a coefficient of determination of 0.9351, an average error of 2.49%, and 100% of the cooling loads that are predicted within an error of 10% or less (Figure 7a). Regarding $\dot{Q}_g^{ce\prime}$, it has a coefficient of determination of 0.9423, an average error of 4.80%, and 77.78% of the heat source loads that are predicted within an error of 10% or less (Figure 7b). Finally, regarding $COP_{th}^{ce\prime}$, it has a coefficient of determination of 0.6852, an average error of 7.24%, and 77.78% of the thermal COPs that are predicted within an error of 10% or less (Figure 7c).

Based on these results, it seems that the CFM and the adapted CE method might be adapted to predict the performances and cooling loads of DEC systems. However, this should be confirmed with experimental tests on systems in a larger operating conditions range and with more experimental points.

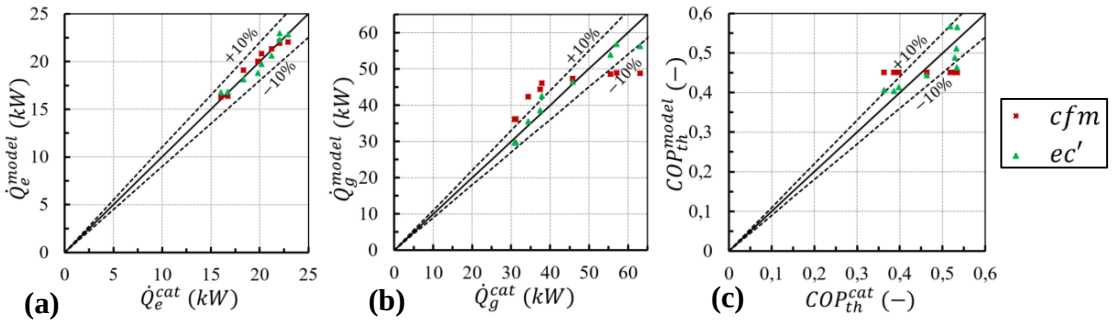

Fig. 7: Comparison between numerical and experimental results for the DEC system

5. Conclusions and perspectives

The present work demonstrated the feasibility of the implementation of the CFM and the adapted CE method (which had until now been exclusively used with absorption chillers) with adsorption chillers and DEC systems. These black box models, that use the external source temperatures as parameters to graphically situate the machine operating conditions, offer the advantages of ease of implementation with dynamic thermal simulation programs such as TRNSYS and a visual representation of the systems' operating regime either through the $\Delta\Delta t'$ or the COP_{carnot}. The main advantage of the COP_{carnot} as a tool to represent the systems' operating conditions is that it is a universal parameter with a physical sense and therefore, a comparison of machines of different nature or geometries in the same domain (COP_{carnot}) is possible. This parameter, however, cannot be fitted for better model prediction accuracy, such as in the case of the $\Delta\Delta t'$ of the adapted CE method, and this might be one of the main reasons why the CFM presented the highest deviations (especially with $\dot{Q}_e$ and $\dot{Q}_g$), limiting its utility for applications in system performance monitoring. A more detailed study is required to highlight the reasons behind these deviations since they might be related to the performances of the individual components (heat and mass exchangers) in the system or to the physical limitations of the theoretical cycle. This might help develop improved black box modeling methods with better accuracy.

6. Acknowledgments

The authors would like to thank the TEC project, funded by Europe's Interreg Caraïbes program, for its support to this research.

7. References

Alahmer, A., Ajib, S., 2020. Solar cooling technologies: State of art and perspectives. Energy Convers. Manag. 214, 112896. https://doi.org/10.1016/J.ENCONMAN.2020.112896

Almasri, R.A., Abu-Hamdeh, N.H., Esmaeil, K.K., Suyambazhahan, S., 2022. Thermal solar sorption cooling systems - A review of principle, technology, and applications. Alexandria Eng. J. 61, 367–402. https://doi.org/10.1016/J.AEJ.2021.06.005

Altamirano, A., Le Pierrès, N., Stutz, B., 2019a. Review of small-capacity single-stage continuous absorption systems operating on binary working fluids for cooling: Theoretical, experimental and commercial cycles. Int. J. Refrig. 106, 350–373. https://doi.org/10.1016/j.ijrefrig.2019.06.033

Altamirano, A., Le Pierrès, N., Stutz, B., Coronas, A., 2021. Performance characterization methods for absorption chillers applied to an NH_3-$LiNO_3$ single-stage prototype. Appl. Therm. Eng. 185, 116435. https://doi.org/10.1016/j.applthermaleng.2020.116435

Altamirano, A., Stutz, B., Le Pierrès, N., Domain, F., 2019b. H2O-LiBr Single-Stage Solar Absorption Air Conditioner with an Innovative Bi-Adiabatic Configuration: Dynamic Model, Nominal Conditions and Typical Day Operation, in: Solar World Congress. Santiago, Chili. https://doi.org/10.18086/swc.2019.55.01

Boudéhenn, F., Bonnot, S., Demasles, H., Lazrak, A., 2014. Comparison of different modeling methods for a single effect water-lithium bromide absorption chiller, in: International Conference on Solar Energy and Buildings, September 16-19. Aix-les-Bains, France. https://doi.org/10.18086/eurosun.2014.07.04

IEA, 2018. World energy outlook. Paris, France.

InvenSor GmbH, 2015. InvenSor LTC 30 e plus technical specifications.

Kühn, A., Ziegler, F., 2005. Operational results of a 10kW absorption chiller and adaptation of the characteristic equation., in: First International Conference on Solar Air Conditioning, October 6-7. Bad-Staffelstein, Germany.

La, D., Dai, Y.J., Li, Y., Wang, R.Z., Ge, T.S., 2010. Technical development of rotary desiccant dehumidification and air conditioning: A review. Renew. Sustain. Energy Rev. 14, 130–147. https://doi.org/10.1016/J.RSER.2009.07.016

Pons, M., Anies, G., Boudehenn, F., Bourdoukan, P., Castaing-lasvignottes, J., Evola, G., Le Denn, A., Le Pierrès, N., Marc, O., Mazet, N., Stitou, D., Lucas, F., 2012. Performance comparison of six solar-powered air-conditioners operated in five places. Energy 46, 471–483. https://doi.org/10.1016/j.energy.2012.08.002

Pons, M., Kodama, A., 1999. Second law analysis of the open cycles for solid desiccant air conditioners, in: Proceeding of ISHPC. Munich, Germany, pp. 389–394.

Robatherm GmbH, 2014. Sorption-Supported Air-Conditioning.

Yazaki Energy Systems Inc., 2018. Yazaki WFC-SC10 Series chiller instalation instructions.

Appendix: Nomenclature

Nomenclature		**Subscripts and superscripts**	
a	characteristic parameter (-)	*0*	Carnot function model y-intercept
b	characteristic parameter (-)	*a*	absorber
c	characteristic parameter (-)	*c*	condenser
CE	characteristic equation	*ec'*	adapted characteristic equation variable
CFM	Carnot function model	*cfm*	Carnot function model variable
COP	coefficient of performance (-)	*e*	evaporator
e	characteristic parameter (-)	*el*	electric
F	Carnot function model parameter (-)	*exp*	experimental
$\dot{Q}$	heat transfer rate (kW)	*g*	generator
r	characteristic parameter (-)	*gl*	global
s'	characteristic parameter (-)	*i*	inlet
T	external temperature (°C)	*int*	intermediate temperature source
$\dot{W}$	power (kW)	*nom*	nominal
		o	outlet
Greek letters		*th*	thermal
α	characteristic parameter (-)		
Δ	differential quantity		
$\Delta\Delta t'$	adapted characteristic temperature difference (K)		
τ	Carnot function model parameter (-)		
ω	Carnot function model parameter (-)		